The Reliability and Operational Test System of a Power Grid with Large-scale Renewable Integration

Jianxue Wang, *Senior Member, IEEE*, Jingdong Wei, Yuchao Zhu, and Xiuli Wang, *Senior Member, IEEE*

***Abstract*—This paper proposes a reliability and operational test system named XJTU-ROTS2017, characterized by large-scale renewable power integration and long-distance transmission. The test system has 38 nodes, 63 lines, 15 transformers and 20 generators in three areas, with peak load 10,421 MW and total installed capacity 16050 MW. Electricity primarily transmits from a resource-rich area to a load area, carrying wind/solar power generation. The determination of component parameters and grid topology is based on design manuals and typical practices. The test system can be conveniently applied to reliability evaluation and operation optimization of composite power systems integrating coal/hydro/solar/wind resources. Finally, the extended applications to AC/DC hybrid power systems and interconnected power systems are discussed.**

***Index Terms*—Test system, large-scale renewable energy, reliability, operation, XJTU-ROTS2017.**

I. Introduction

The worsening situations of an energy crisis and environmental pollution pose higher requirements on clean production and renewable energy utilization, promoting the rapid worldwide development of wind and solar energy [1]. There exist two main trends in renewable energy development, i.e., small-scale distributed generation and large-scale centralized generation. As the most representative country in terms of centralized renewable generation, China has a number of 10 GW-size wind power and photovoltaic bases, and its transmission lines between resource bases and load centers are often hundreds or thousands of kilometers long [2]. Due to its intermittency and fluctuation, renewable energy has obvious influences on power system planning and operations. Therefore, a test system characterized by large-scale renewable integration and long distance transmission is urgently needed.

The typical test systems for IEEE-Reliability Testing, IEEE-RTS24 [3] and IEEE-RTS96 [4], were published in 1979 and 1999, respectively. The two systems are primarily employed for power system reliability evaluation, whose widespread utilization has significantly promoted relevant research. Many of the power system features at that stage are included, such as small generating capacity, high failure rates of generation units and considerable redundancy of transmission systems.

Furthermore, TH-TRS was designed in 2000, which has larger generating capacity and highlights system interconnection [5]. But some features of modern power systems need to be reflected more appropriately, such as renewable energy integration. The newest research extends the IEEE 118-Bus test system to NREL-118, which reflects features of decentralized integration and consumption of renewable energy, and robust regulation ability brought by the high proportion of gas generation [6] in North America. However, the IEEE test systems are based on special power systems, which are very different from the situations of actual power systems, even if modified. The characteristics of the actual power systems, such as the typical mode of large-scale integration and long distance transmission of renewable energy, and system inflexibility brought about by the high proportion of coal-fired generation, are not easy to be embodied by slightly modifying existing IEEE test systems. Hence, a new test system that could cover the situations of actual power systems and provide a standardized platform for research, is worth investigation.

This paper designs a test system named XJTU-ROTS2017 from scratch, which illustrates the characteristics of the actual power systems, and works as a typical example for research under the scenario of a high proportion of renewable energy. This test system improves the existing test systems, highlights the characteristics of large-scale wind/solar power integration, as well as providing testing examples for operational optimization of power systems with renewable integration. In addition, considering the widespread use of test systems in reliability evaluation, reliability data is also incorporated in XJTU-ROTS2017, which offers convenient application to both reliability evaluation and operational optimization.

II. Overall Conditions of XJTU-ROTS2017

A. Principles of Test System Design

The design principles of test system XJTU-RPTS2017 are summarized as follows:

1) Compositions of Voltage Levels

In order to demonstrate high voltage levels, large-scale renewable integration and long-distance transmission, the highest voltage level is chosen as 500 kV. It should be noted that the highest voltage level is similar to that of main transmission networks worldwide, while higher than that in IEEE-RTS24 (238 kV). Meanwhile, the voltage level of transmission networks in the load area is selected as 220 kV. Hence, the

Manuscript received December 29, 2017; revised July 25, 2018; accepted September 7, 2018. Date of online publication November 30, 2019; date of current version April 17, 2020.

J. X. Wang (corresponding author, e-mail: jxwang@mail.xjtu.edu.cn.), J. D. Wei, Y. C. Zhu and X. L. Wang are with the School of Electrical Engineering, Xi'an Jiaotong University, Xi'an 710049, China.

DOI: 10.17775/CSEEJPES.2017.01300

500 kV voltage level realizes the long distance transmission of large-scale renewable energy resources, while the 220 kV voltage level satisfies supply and demand needs of resource-rich areas and load areas in the grid. In addition, the voltage at the transformer low voltage side is chosen as 35 kV.

2) Power Grid Structure

The overall power grid structure should represent long-distance power transmission from resource-rich areas to load areas. The typical structures in practice need to be investigated and incorporated into the test system [7], [8]. Grid structure design follows two basic rules: 1) The capacity and number of lines and transformers should be selected according to design rules in practice. 2) The design of the grid topology takes into account N-1 criteria.

B. System Overview and Generation Composition

For convenience, the electric quantities in this paper have both actual values and per unit values. The reference capacity is 100 MVA, and the reference voltages for the 500 kV and 220 kV grids are chosen as 525 kV and 230 kV, respectively.

The general parameters of XJTU-ROTS2017 are shown in Table I.

TABLE I
GENERAL PARAMETERS OF XJTU-ROTS2017

Nodes	Lines	Trans-formers	Gener-ators	Loads	Annual Peak Load	Total Installed Capacity
38	63	15	20	30	10421 MW	16050 MW

Figure 1 shows the installed capacity ratio of each type of power unit. Among them, the installed capacity of coal-fired power units accounts for 2/3, which reflects the power structure dominated by coal-fired generation [9]. It is necessary to point out that the coal-fired generators have relatively high startup and shutdown costs, and require the minimum output in operation. Consequently, the large ratio of coal-fired thermal power leads to the lack of flexibility in power system operations, which is unfavorable to large-scale renewable energy consumption. In comparison, large-scale renewable integration and system inflexibility brought by a high proportion of coal-fired generation are not reflected in IEEE test systems.

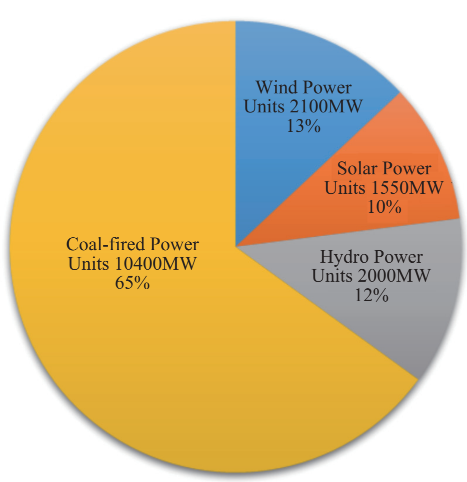

Fig. 1. Installed capacity ratio of each type of power unit in XJTU-ROTS2017.

C. Test System Grid Topology

The grid topology of the test system is illustrated in Fig. 2. It can be divided into a resource-rich area (Area A), 500 kV area (Area B) and load area (Area C). The connection points of wind/solar/coal-fired/hydro power generation, transmission line lengths (depicted by numbers on the lines) and node voltage level information are also illustrated in Fig. 2.

The numbering for each node is unified. The transformer nodes contain different voltage levels, thus corresponding to multiple buses. To distinguish these buses with the same transformer, this paper uses suffixes like-H, -M, -L, which are corresponding to the high/medium/low voltage side of the transformer, respectively. For example, C22H stands for the high voltage side of the transformer node C22.

Long-distance transmission of renewable energy is illustrated in the grid topology. The longest line is 270 km, and the longest distance from the resource-rich area (Area A) to load area (Area C) reaches up to 700–800 km. Compared with existing test systems, it is more challenging to coordinate renewable generation and consumption in wide ranges from the view of the whole system.

III. DATA OF POWER GENERATION

A. Data of Renewable Energy Generation

Considering the influence of seasonal variability and short-time intermittency on system operations and reliability evaluation, hourly time series information of renewable output is critical [6].

Wind speed data from NREL [10] and illumination intensity data generated by Homer software are transferred to wind/solar power output data. These data are also revised according to the average utilization hours of solar/wind power.

Wind farms located at A1 adopt 1# wind power data (with most abundant wind resources), wind farms at A3, A4 and A5 employ 2# wind power data, and the wind farm at C35 uses 3# wind power data (with least abundant wind resources). Also, the photovoltaic power station at A2 uses 1# solar power data (with most abundant photovoltaic resources), photovoltaic power stations at A6 and A7 apply 2# solar power data, and the photovoltaic power station at C36 adopts 3# solar power data.

Take the 1# solar/wind power data as an example, Figs. 3 and 4 illustrate the daily output curves of wind and solar power in four seasons in a year, respectively.

Compared with NREL-118, which is characterized by high renewable penetration, the design in this paper highlights the typical mode of large-scale renewable integration in forms of large renewable power stations. In comparison, the typical mode of renewable large-scale integration and long distance transmission of renewable energy, are not evident in IEEE test systems.

Table II gives information about wind/solar power generation. The corresponding power factor of renewable power can be set as some certain value in the calculation, such as 1.0 or 0.98.

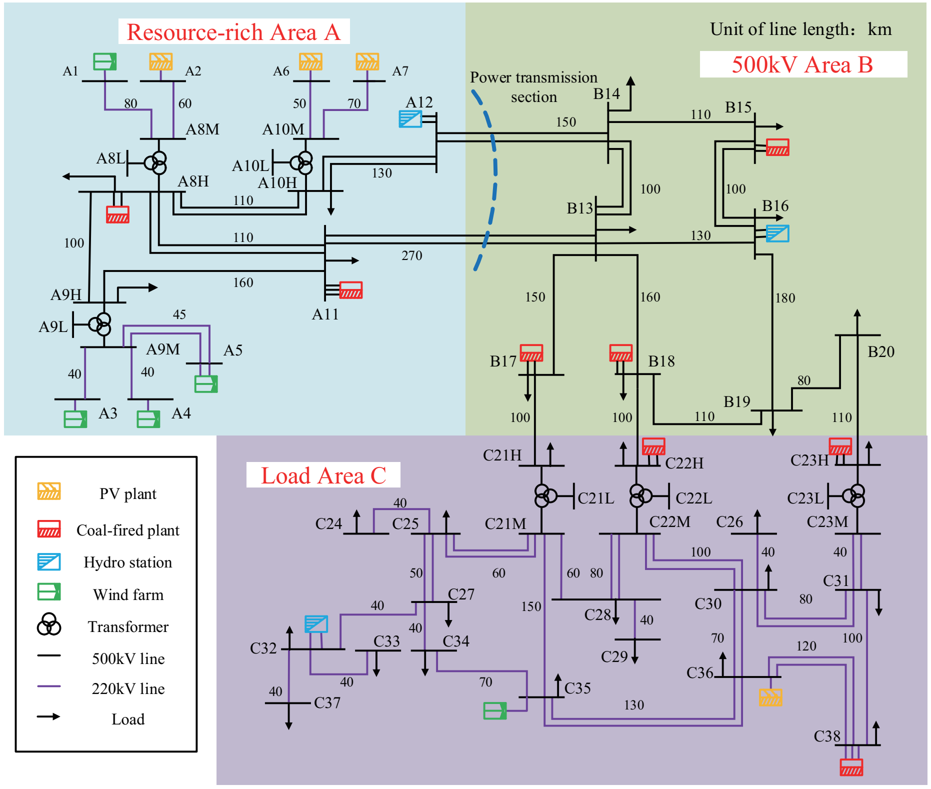

Fig. 2. Grid topology of XJTU-ROTS2017.

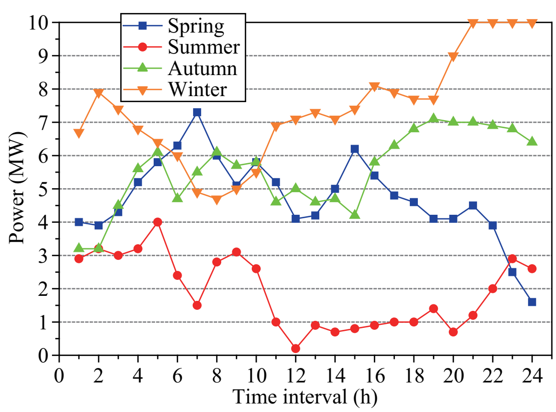

Fig. 3. Typical output of 1# wind power during four seasons.

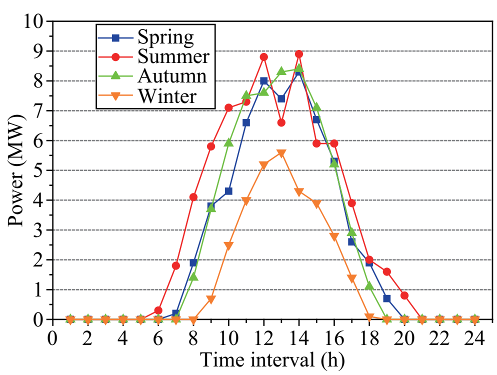

Fig. 4. Typical output of 1# solar power during four seasons.

TABLE II
DATA OF RENEWABLE ENERGY GENERATION

Number	Generation Type	Node	Installed Capacity (MW)
G1	Wind Power	A1	400
G2	Wind Power	A3	400
G3	Wind Power	A4	400
G4	Wind Power	A5	800
G5	Wind Power	C35	100
G6	Photovoltaic Power	A2	500
G7	Photovoltaic Power	A6	500
G8	Photovoltaic Power	A7	500
G9	Photovoltaic Power	C36	50

B. Data of Hydropower Station

Table III gives the basic data of hydro stations, including unit capacity, number of installed units, operating range of reactive power, ramp rate and monthly generation. In this paper, the rainy season is from April to September, and the dry season is from January to March and from October to December. G10 is a hydropower station capable of long-term regulation (with a large reservoir), and G11 and G12 are the hydropower stations with less regulation ability. Some hydropower stations (such as G11) can also be set as a pumped storage power station in a future study.

Table IV gives the reliability data of the hydro power generating units by reference to IEEE-RTS24 [3] and the statistical data of actual power system operation.

C. Data of Coal-fired Power Plant

Table V gives the data of coal-fired power plants, including unit capacity, number of installed units, operating range of

TABLE III
DATA OF HYDROPOWER PLANTS

Number	Bus Name	Unit Capacity (MW)	Number of Installed Units	Operating Range of Reactive Power (Mvar)	Ramp Rate (MW/min)	Maximum Monthly Generation of Hydropower Station in Rainy Season (GWh)	Maximum Monthly Generation of Hydropower Station in Dry Season (GWh)
G10	A12	200	4	[−50, 124]	80	290	210
G11	B16	200	4	[−50, 124]	60	270	170
G12	C32	200	2	[−50, 124]	60	120	90

TABLE IV
RELIABILITY DATA OF HYDROPOWER GENERATING UNITS

Number	Forced Outage Rate	MTTF (h)	MTTR (h)	Scheduled Maintenance (Weeks/Year)
G10	0.0015	8000	12	4
G11	0.0015	8000	12	4
G12	0.0012	8300	10	4

TABLE V
DATA OF COAL-FIRED POWER PLANTS

Number	Bus Name	Unit Capacity (MW)	Number of Installed Units	Operating Range of Reactive Power (Mvar)	Minimum Output (MW)	Ramp Rate (MW/min)	Minimum Up Time (h)	Minimum Down Time (h)	Start-up and Shut-down Cost (10^4 RMB)
G13	A8H	600	2	[−150, 372]	240	18	8	5	140
G14	A11	600	4	[−150, 372]	240	18	8	5	140
G15	B15	600	2	[−150, 372]	240	18	8	5	140
G16	C22H	200	6	[−50, 124]	90	4	5	4	50
G17	C23H	200	6	[−50, 124]	90	4	5	4	50
G18	C38	200	4	[−50, 124]	90	4	5	4	50
G19	B17	300	4	[−75, 186]	130	6	6	4	100
G20	B18	300	4	[−75, 186]	130	6	6	4	100

reactive power, minimum output, ramp rate, minimum up time, minimum down time, and start-up and shut-down costs. Considering the current refit of some thermal units, there are some differences between ramp rates. Compared with reliability systems, this test system provides more detailed information.

Table VI gives the reliability data of the coal-fired power generating units also by reference to the statistical data of actual power system operation.

TABLE VI
RELIABILITY DATA OF COAL-FIRED POWER UNITS

Number	Forced Outage Rate	MTTF (h)	MTTR (h)	Scheduled Maintenance (Weeks/Year)
G13	0.0036	7850	28	6
G14	0.0038	7850	30	6
G15	0.0039	7850	31	6
G16	0.0055	3235	18	4
G17	0.0068	3235	22	4
G18	0.0061	3235	20	4
G19	0.0045	5730	26	5
G20	0.0043	5730	25	5

Table VII gives the unit coal consumption data of coal-fired power units. The calculation formula on the coal consumption of the coal-fired unit is $B(P) = aP^2 + bP + c$. The coefficients a, b and c are shown in Table VII, which can be used in larger research such as economic dispatch.

It should be noted that all the thermal power plants in this paper are assumed to be coal-fired plants. Actually, gas generation and oil generation can easily be included by replacing part of the coal-fired generation units with gas-fired or oil-fired generation units, whose consumption parameters can be given according to NREL-118 [6].

TABLE VII
FUEL CONSUMPTION DATA OF COAL-FIRED POWER UNITS

Number	Coefficient of Coal Consumption Per Unit a (t/MW^2·h)	Coefficient of Coal Consumption Per Unit b (t/MW·h)	Coefficient of Coal Consumption Per Unit c (t/h)
G13	0.000017	0.2350	23.0194
G14	0.000017	0.2530	21.0194
G15	0.000017	0.2600	20.0194
G16	0.000092	0.2499	13.6349
G17	0.000091	0.2540	12.9950
G18	0.000092	0.2382	14.2485
G19	0.000160	0.2317	10.1872
G20	0.000150	0.2299	10.6686

IV. LOAD DATA

The data of load at each node in the peak load period is given in Table VIII, where the total peak load reaches up to 10,421 MW. The distribution laws of hourly load curves follow the load model in IEEE-RTS24 [3], which can be obtained by multiplying the peak load by load distribution coefficients. In this way, typical hourly load curves of certain days during the four seasons in a year could be generated, as shown in Fig. 5.

The detailed load types, including large industrial load, metallurgical industry load, urban power load, rural power load, as well as composite load consisting of various loads, are given in Table VIII, which is fundamental to reliability evaluation and operational optimization with more precision.

In a future study, flexible load, such as electric vehicles and energy storage stations, should be taken into consideration. Some research might need data about the Value of Lost Load (VoLL), which can be referenced in [11].

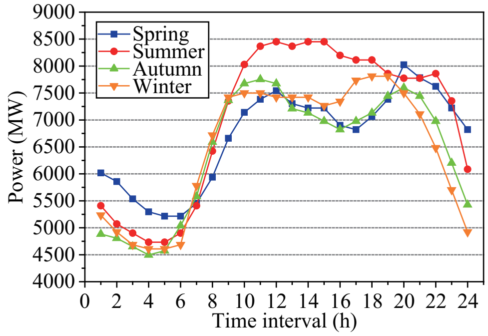

Fig. 5. Typical hourly load curves for certain days in a year.

TABLE VIII
NODAL LOAD DATA IN PEAK LOAD PERIOD

Number	Bus Name	Peak Load (MW)	Load Type	Power Factor
1	A8H	60	Composite Load	0.90
2	A9H	200	Composite Load	0.90
3	A10H	300	Composite Load	0.90
4	A11	64	Composite Load	0.90
5	B13	1400	Composite Load	0.90
6	B14	1200	Composite Load	0.90
7	B15	614	Composite Load	0.90
8	B16	630	Composite Load	0.90
9	B17	84	Composite Load	0.90
10	B18	390	Composite Load	0.90
11	C21H	320	Composite Load	0.90
12	C22H	284	Composite Load	0.90
13	B19	610	Composite Load	0.90
14	B20	800	Composite Load	0.90
15	C23H	384	Composite Load	0.90
16	C24	110	Rural Power Load	0.85
17	C25	240	Large Industrial Load	0.92
18	C26	96	Rural Power Load	0.85
19	C27	120	Metallurgical Industry Load	0.80
20	C28	340	Large Industrial Load	0.92
21	C29	102	Rural Power Load	0.85
22	C30	150	Large Industrial Load	0.92
23	C31	172	Metallurgical Industry Load	0.80
24	C32	140	Metallurgical Industry Load	0.80
25	C33	96	Rural Power Load	0.85
26	C34	300	Urban Power Load	0.90
27	C35	460	Large Industrial Load	0.92
28	C36	344	Large Industrial Load	0.92
29	C37	145	Urban Power Load	0.90
30	C38	266	Large Industrial Load	0.92

V. BRANCH DATA

A. Data of Transmission Lines

Table IX gives the basic parameters and reliability data of transmission lines. The line element model uses a π type equivalent circuit [12], R, X denote line resistance and reactance, $B_{50\%}$ represents half of transmission line grid-to-earth capacitance, and $P_{\max}$ indicates the maximum transmission capacity of each line.

The maximum capacity of the transmission section, which generally consists of multiple adjacent lines, is also an important factor to consider in power system operations. In this system, the key transmission section, whose maximum capacity is set as 56.82 (p.u.), is formed by two double-circuit lines, i.e. A11–B13 and A12–B14 (as shown in Fig. 2).

B. Data of Transformers

The component model of the transformer is referred to in literature [12]. Tables X and XI show the transformer data in the test system [7]. There are three sets of three-winding transformers operating in parallel of A8, A9, A10 and two sets of three-winding transformers operating in parallel of C21, C22, C23.

If reactive voltage optimization is required, the transformers can be chosen as OLTC (On Load Tap Changing) transformers, whose taps at high and medium voltage sides are both $\pm\, 8 \times 1.25\%$.

C. Data of Reactive Power Compensation

The low-voltage side bus of each transformer is configured with capacitor groups and reactor groups. Table XII shows reactive compensation data of capacitors and reactors in substations A8–A10 and C21–C23. Other 500 kV substations in the grid topology can be configured referring to Table XII. The exemplary configuration of 220 kV substations is with three 10 Mvar capacitors and one 12 Mvar reactor.

VI. SYSTEM APPLICATIONS AND EXTENSIONS

A. Comprehensive Utilization of the Test System

In the test system, most settings totally follow the design manuals or actual designs, and typical characteristics of the actual operating conditions are considered. Therefore, the test system is capable of offering a standardized platform to inspect the feasibility and superiority of the theory or method.

It could be utilized for the reliability evaluation of a generation system or composite system. It could provide relevant parameters for state sampling and sequential sampling. Also, it is applicable to power flow, optimal power flow and economic dispatch.

In addition to reliability evaluation and operational optimization of the power system with renewable energy, the test system data can also be directly applied to other research fields, e.g., unit commitment, reactive power optimization, power market and production simulation.

B. Extended Applications of the Test System

The future adaptability of XJTU-ROTS2017 is also taken into account, which can be extended in the following aspects:

1) Extension of the Unit Types

In this paper, the type of generators can be further extended. Coal-fired generators can be replaced by nuclear/gas/oil-fired generators or CHP units, photovoltaic stations can be replaced by photothermal power stations, and hydropower stations can be replaced by pumped storage power stations or energy storage power stations. Each node may be connected with different types of generators. For example, it can be connected with a hydro-photovoltaic power station [13].

2) Expansion of AC System to AC/DC Hybrid System

The system has reserved expansion interfaces for DC lines, as illustrated in Fig. 6. In the grid topology, the nodes A8 and B19 are prepared for future DC points. A point-to-point DC line could be built between the power center and load center, thus expanding the system to an AC-DC hybrid system.

TABLE IX
BASIC PARAMETERS AND RELIABILITY DATA OF TRANSMISSION LINES

Number	From Bus	To Bus	Length (km)	R (p.u.)	X (p.u.)	$B_{50\%}$ (p.u.)	Permanent Outage Rate (Outages/Year)	Permanent Outage Duration (h)*	$P_{\max}$ (p.u.)
L1	A1	A8M	80	0.001161	0.008703	0.414039	0.0752	4	5.33
L2	A2	A8M	60	0.000871	0.006527	0.31053	0.0564	4	5.33
L3	A3	A9M	40	0.00058	0.004351	0.20702	0.0376	4	5.33
L4	A4	A9M	40	0.00058	0.004351	0.20702	0.0376	4	5.33
L5/L6	A5	A9M	45	0.000653	0.004895	0.232897	0.0423	4	5.33
L7	A6	A10M	50	0.000726	0.005439	0.258775	0.047	4	5.33
L8	A7	A10M	70	0.001016	0.007615	0.362285	0.0658	4	5.33
L9	A8H	A9H	100	0.00098	0.009905	0.563897	0.094	6	20.45
L10/L11	A8H	A10H	110	0.001078	0.010895	0.620286	0.1034	6	20.45
L12/L13	A8H	A11	110	0.001078	0.010895	0.620286	0.1034	6	20.45
L14	A9H	A11	160	0.001567	0.015848	0.902235	0.1504	6	20.45
L15/L16	A10H	A12	130	0.001088	0.014959	0.853625	0.141	6	24.34
L17/L18	A11	B13	270	0.001959	0.026926	1.536525	0.2138	6	24.34
L19/L20	A12	B14	150	0.001088	0.014959	0.853625	0.141	6	24.34
L21/L22	B13	B14	100	0.00098	0.009905	0.563897	0.094	6	20.45
L23	B13	B16	130	0.001273	0.012876	0.733066	0.1222	6	20.45
L24	B13	B17	150	0.001469	0.014857	0.845845	0.141	6	20.45
L25	B13	B18	160	0.001567	0.015848	0.902235	0.1504	6	20.45
L26	B14	B15	110	0.001078	0.010895	0.620286	0.1034	6	20.45
L27/L28	B15	B16	100	0.00098	0.009905	0.563897	0.094	6	20.45
L29	B16	B19	180	0.001763	0.017829	1.015014	0.1692	6	20.45
L30	B17	C21H	100	0.00098	0.009905	0.563897	0.094	6	20.45
L31	B18	C22H	100	0.00098	0.009905	0.563897	0.094	6	20.45
L32	B18	B19	110	0.001078	0.010895	0.620286	0.1034	6	20.45
L33	B19	B20	80	0.000784	0.007924	0.451117	0.0752	4	20.45
L34	B20	C23H	110	0.001078	0.010895	0.620286	0.1034	6	20.45
L35/L36	C21M	C25	60	0.000871	0.006527	0.31053	0.0564	4	5.33
L37	C21M	C28	60	0.000871	0.006527	0.31053	0.0564	4	5.33
L38	C21M	C35	150	0.002177	0.016318	0.776324	0.141	6	5.33
L39/L40	C22M	C28	80	0.001161	0.008703	0.414039	0.0752	4	5.33
L41/L42	C22M	C30	100	0.001451	0.010879	0.517549	0.094	6	5.33
L43/L44	C23M	C31	40	0.00058	0.004351	0.20702	0.0376	4	5.33
L45	C24	C25	40	0.000784	0.004418	0.203816	0.0376	4	4.48
L46/L47	C25	C27	50	0.00098	0.005523	0.25477	0.047	4	4.48
L48	C26	C30	40	0.000784	0.004418	0.203816	0.0376	4	4.48
L49	C27	C32	40	0.000784	0.004418	0.203816	0.0376	4	4.48
L50	C27	C34	40	0.000784	0.004418	0.203816	0.0376	4	4.48
L51	C28	C29	40	0.000784	0.004418	0.203816	0.0376	4	4.48
L52/L53	C30	C31	80	0.001567	0.008836	0.407632	0.0752	4	4.48
L54/L55	C30	C36	70	0.001371	0.007732	0.356678	0.0658	4	4.48
L56	C31	C38	100	0.001959	0.011045	0.50954	0.094	6	4.48
L57	C32	C33	40	0.000784	0.004418	0.203816	0.0376	4	4.48
L58	C32	C37	40	0.000784	0.004418	0.203816	0.0376	4	4.48
L59	C34	C35	70	0.001371	0.007732	0.356678	0.0658	4	4.48
L60/L61	C35	C36	130	0.002547	0.014359	0.662402	0.1222	6	4.48
L62/L63	C36	C38	120	0.002351	0.013255	0.611448	0.1128	6	4.48

*The permanent outage duration of lines is estimated according to engineering experience, which will be updated and improved by statistical data in the future.

TABLE X
TRANSFORMER VOLTAGE LEVEL AND CAPACITY

Number	High Voltage Bus	Medium Voltage Bus	Low Voltage Bus	High/Medium/Low Rated Voltage (kV)	Capacity (MVA)	Permanent Outage Rate (Outages/Year)	Permanent Outage Duration (h)**
T1 $\sim$ T3	A8H	A8M	A8L	525/230/35 kV	750	0.00136	12
T4 $\sim$ T6	A9H	A9M	A9L	525/230/35 kV	750	0.00136	12
T7 $\sim$ T9	A10H	A10M	A10L	525/230/35 kV	750	0.00176	12
T10 $\sim$ T11	C21H	C21M	C21L	525/230/35 kV	750	0.00182	10
T12 $\sim$ T13	C22H	C22M	C22L	525/230/35 kV	750	0.00182	10
T14 $\sim$ T15	C23H	C23M	C23L	525/230/35 kV	750	0.00182	10

**The permanent outage rates of transformers are estimated based on engineering experience, which will be updated and improved by statistical data in the future.

TABLE XI
TRANSFORMER IMPEDANCE PARAMETERS

Number	*R1* (p.u.)	*X1* (p.u.)	*R2* (p.u.)	*X2* (p.u.)	*R3* (p.u.)	*X3* (p.u.)
T1 $\sim$ T9	0.000106	0.017527	0.000058	−0.001530	0.000420	0.044073
T10 $\sim$ T15	0.000090	0.020473	0.000079	−0.001830	0.000524	0.047500

TABLE XII
DATA OF CAPACITORS/REACTORS

Bus Name	Voltage Level	Compensating Capacitor of Each Transformer (Mvar)	Compensating Reactor of Each Transformer (Mvar)
A8L ∼ A10L	35 kV	2 × 60	2 × 60
C21L ∼ C23L	35 kV	2 × 60	2 × 60

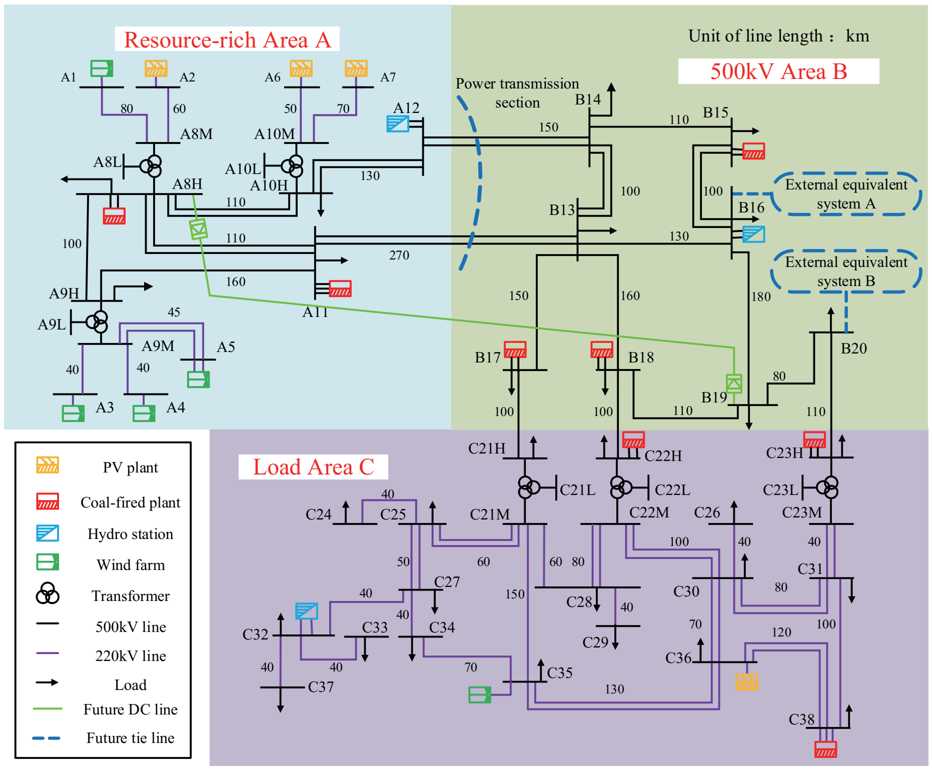

Fig. 6. Extended Applications of XJTU-ROTS2017.

3) Expansion of Single System to Multiple Interconnected Systems

In the grid topology, the nodes (such as B16 and B20) are reserved for future system expansion, which helps to realize power exchange between XJTU-ROTS2017 and external systems. By connecting the reserved nodes to the corresponding extern nodes, the system proposed in this paper can be connected to other typical test systems such as IEEE-RTS24, IEEE-RTS96, IEEE 30-bus test system, and IEEE 118-bus test system, thus forming a more complicated test system.

In addition, the installed capacity of renewable energy can be enlarged (such as over 50% total installed capacity) to identify reliability and operational problems with high-proportion renewable integration.

VII. Conclusion

In this paper, a virtual test system named XJTU-ROTS2017 is designed as a test example for reliability and operational research. In particular, the test system is characterized in that

1) It demonstrates large-scale renewable integration.

2) It highlights long-distance transmission.

3) It reflects the power supply structure dominated by coal-fired generation.

4) It could be applied to both reliability evaluation and operational optimization.

Furthermore, the proposed test system has good adaptability in designing more complex systems, such as AC/DC hybrid power systems and interconnected power systems.

Acknowledgment

It is really a great challenge to design a complete and virtual test system from scratch. Sincere thanks go to Dr. Fu Xu for his valuable suggestions. His planning and design working experience helped the study proceed smoothly. In addition, thanks go to Tianhui Zhao and Minghui Zhu, who also contributed some calculation verification to this study. For the detailed wind/solar power data, the calculation results of reliability and operations, as well as the improved data involved in this paper, please visit the website http://gr.xjtu.edu.cn/web/jxwang/xjtu-rots.

References

[1] R. Baños, F. Manzano-Agugliaro, F. G. Montoya, C. Gil, A. Alcayde, and J. Gómez, "Optimization methods applied to renewable and sustainable energy: A review," in *Renewable & Sustainable Energy Reviews*, vol. 15, pp. 1753–1766, May 2011.

[2] B. Sun, Y. Yu and C. Qin, "Should China focus on the distributed development of wind and solar photovoltaic power generation? A comparative study," in *Applied Energy*, vol. 185, pp. 421–439, Jan. 2017.

[3] P. M. Subcommittee, "IEEE Reliability Test System," in *IEEE Transactions on Power Apparatus & Systems*, vol. PAS-98, pp. 2047–2054, Nov. 1979.

[4] C. Grigg, P. Wong, P. Albrecht, R. Allan, M. Bhavaraju, R. Billinton, Q. Chen, C. Fong, S. Haddad, S. Kuruganty, W. Li, R. Mukerji, D. Patton, N. Rau, D. Reppen, A. Schneider, M. Shahidehpour, and C. Singh, "The IEEE Reliability Test System-1996. A report prepared by the Reliability Test System Task Force of the Application of Probability Methods Subcommittee," in *IEEE Transactions on Power Systems*, vol. 14, no. 3, pp. 1010–1018, Aug. 1999.

[5] Y. Guo, L. Cheng, "Reliability test system for composite generation and transmission system in CHINA [TH-RTS2000]," in *Automation of Electric Power Systems*, vol. 25, no. 20, pp. 35–40, Oct. 2001.

[6] I. Pena, C. Brancucci and B. M. Hodge, "An extended IEEE 118-bus test system with high renewable penetration," in *IEEE Transactions on Power Systems*, vol. PP, p. 1–9, 2017.

[7] P. Hines, S. Blumsack, E. C. Sanchez, and C. Barrows, "The topological and electrical structure of power grids," in *Hawaii International Conference on System Sciences*, 2010, pp. 1–10.

[8] Northwest Electric Power Design Institute. Design manual of electric power engineering. Beijing: China Electric Power Press, 1996.

[9] Y. Li, "Dynamics of clean coal-fired power generation development in China," in *Energy Policy*, vol. 51, pp. 138–142, Dec. 2012.

[10] NREL (2015), "NREL: Transmission Grid Integration- Wind Integration National Dataset (WIND) Toolkit,". [Online]. Available: http://www.nrel.gov/electricity/transmission/wind_toolkit.html.

[11] London Economics. The Value of Lost Load (VoLL) for Electricity in Great Britain, 2013. https://www.ofgem.gov.uk/ofgem-publications/82293/london-economics-value-lost-load-electricity-gbpdf. Available Date: 2017-11-08.

[12] P. S. Kundur, Power system stability and control. New York: McGraw-Hill Professional, 1994.

[13] W. Fang, Q. Huang, S. Huang, J. Yang, E. Meng, and Y. Li, "Optimal sizing of utility-scale photovoltaic power generation complementarily operating with hydropower: A case study of the world's largest hydro-photovoltaic plant," in *Energy Conversion & Management*, vol. 136, no. 15, pp. 161–172, Mar. 2017.

Jianxue Wang received his B.S., M.S., and Ph.D. degrees in Electrical Engineering from Xi'an Jiaotong University, Xi'an, China, in 1999, 2002, and 2006, respectively.

He is currently a Professor in the School of Electrical Engineering, Xi'an Jiaotong University. His current research interests include power system planning and operations, microgrid planning and operations, and the electricity market.

Jingdong Wei received his B.S. degree in Electrical Engineering from Shenyang University of Technology, Shenyang, China in 2014 and is currently pursuing his Ph.D. degree in Electrical Engineering at Xi'an Jiaotong University, Xi'an, China.

His research interests include multi-energy system operations and planning, multi-energy microgrid planning and integrated energy system dispatch.

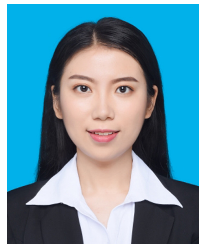

Yuchao Zhu received her B.S. degree in Electrical Engineering from Xi'an Jiaotong University, Xi'an, China in 2016 and is currently pursuing her M.S. degree in Electrical Engineering at Xi'an Jiaotong University, Xi'an, China.

Her research interests include the integration of renewable energy and power markets.

Xiuli Wang received her M.S. and Ph.D. degrees in Electrical Engineering from Xi'an Jiaotong University, Xi'an, China, in 1985 and 1997, respectively. She has been a Professor in the Electrical Engineering Department, Xi'an Jiaotong University since 2001.

Her research interests include power system planning, power market, power system reliability, and HVDC transmission.